Vol 15 No 2, February 2006
1009-1963/2006/15(02)/0437-07

Chinese Physics

© 2006 Chin. Phys. Soc.
and IOP Publishing Ltd

# Adaptive split-step Fourier method for simulating ultrashort laser pulse propagation in photonic crystal fibres*

Li Shu-Guang(李曙光)[a)b)†], Xing Guang-Long(邢光龙)[a)], Zhou Gui-Yao(周桂耀)[a)b)], Han Ying(韩 颖)[a)], Hou Lan-Tian(侯蓝田)[a)b)], Hu Ming-Lie(胡明列)[c)], Li Yan-Feng(栗岩锋)[c)], and Wang Qing-Yue(王清月)[c)]

[a)] *Institute of Infrared Optical Fibers and Sensors, College of Science, Yanshan University, Qinhuangdao 066004, China*
[b)] *Key Laboratory of Metastable Materials Science and Technology, Yanshan University, Qinhuangdao 066004, China*
[c)] *Key Laboratory of Optoelectronic Information Technical Science, Ministry of Education, College of Precision Instrument and Optoelectronics Engineering, Tianjin University, Tianjin 300072, China*

(Received 10 June 2005; revised manuscript received 8 November 2005)

In this paper, the generalized nonlinear Schrödinger equation (GNLSE) is solved by an adaptive split-step Fourier method (ASSFM). It is found that ASSFM must be used to solve GNLSE to ensure precision when the soliton self-frequency shift is remarkable and the photonic crystal fibre (PCF) parameters vary with the frequency considerably. The precision of numerical simulation by using ASSFM is higher than that by using split-step Fourier method in the process of laser pulse propagation in PCFs due to the fact that the variation of fibre parameters with the peak frequency in the pulse spectrum can be taken into account fully.

**Keywords:** photonic crystal fibre, ultrashort laser pulse propagation, adaptive split-step Fourier method

**PACC:** 7155J, 7830, 3320K

## 1. Introduction

In recent years, there has been extensive interest in a new technique based on the use of photonic crystal fibre (PCF) as a nonlinear medium for supercontinuum (SC) generation.[1−15] Studies about ultrashort laser pulses propagating in PCFs and SC generation have become an important branch in the nonlinear optics field. Solving the generalized nonlinear Schrödinger equation (GNLSE) or nonlinear Schrödinger equation (NLSE) is important for understanding the ultrashort laser pulse interaction with the fibres. Zhu and Brown[5] have studied the effect of pulse frequency chirp on the supercontinuum bandwidth in PCFs by GNLSE. Schreiber *et al*[6] have reported the generation of a high average power flat supercontinuum using a compact ytterbium-doped fibre and simulated the experimental results by GNLSE.

In this paper, we propose an adaptive split-step Fourier method (ASSFM) in order to improve the precision of numerical simulation for the pulse propagation and evolution in PCFs. Based on the traditional SSFM, the adaptive idea is applied to simulate ultrashort pulse propagation in PCFs in this method. The variations of fibre parameters corresponding to the pulse spectrum peak with the transmission distance can be taken into account adequately in this method. The reliability of this method is validated by comparison between simulation and experimental results. Furthermore, ultrashort pulses propagating in the different dispersion regimes of PCFs are simulated. In particular, the nonlinear mechanism and supercontinuum characteristics in the propagation process are analysed.

## 2. Basic theory

*Project supported by the State Key Development Program for Basic Research of China (Grant No 2003CB314905), the National High Technology Development Program of China (Grant No 2003AA311011) and Postdoctoral Workstation Research Program of Gulf Security Technology Co. Ltd.

†E-mail: shuguangli@ysu.edu.cn

### 2.1. The basic equation governing pulse transmission in a fibre

Pulse propagation in a fibre is governed by the GNLSE. It is described as[16,17]

$$\frac{\partial A}{\partial z}+\frac{\alpha(\omega)}{2}A+\left(\sum_{n\geq 2}\beta_n(\omega)\frac{\mathrm{i}^{n-1}}{n!}\frac{\partial^n}{\partial T^n}\right)A$$
$$=\mathrm{i}\gamma(\omega)\left[|A|^2A+\frac{\mathrm{i}}{\omega_0}\frac{\partial(|A|^2A)}{\partial T}-T_{\mathrm{R}}A\frac{\partial|A|^2}{\partial T}\right]. \quad (1)$$

Here, $A$ is the electric field amplitude, $z$ is the longitudinal coordinate along the fibre, $T=t-\beta_1 z$ is the time in a reference frame travelling with the pump light, $\beta_n(\omega_0)=(\mathrm{d}^n\beta/\mathrm{d}\omega^n)_{\omega=\omega_0}$ is the $n$th-order dispersion coefficient at the central frequency $\omega_0$, $\alpha(\omega_0)$ is the fibre loss, $\gamma(\omega_0)=\dfrac{n_2\omega_0}{cS_{\mathrm{eff}}}$ is the nonlinear coefficient, where $n_2$ is the nonlinear refractive index of fused-silica glass and $S_{\mathrm{eff}}$ is the effective mode area of the fibre, and $T_{\mathrm{R}}$ is the time parameter corresponding to the delayed Raman response.

### 2.2. The basic idea and process about the ASSFM

The adaptive method is an important method that has been used extensively in signal obtaining processes. We have used adaptive deconvolution to obtain information in petroleum well logging.[18] The ASSFM is used for the first time, so far as we know, to improve the precision of numerical simulation for the pulse propagation and evolution in PCFs in this paper.

The basic idea of the ASSFM is described as follows. On the one hand, it is well known that the PCF parameters $\alpha(\omega)$, $\beta_n(\omega)$ and $\gamma(\omega)$ are functions of $\omega$. These parameters can vary greatly with the pulse frequency because of their high sensitivity to the fibre structure.[19−22] On the other hand, the soliton self-frequency shift varies with the transmission distance $z$ when the pulses propagate in the PCF. For these reasons, the GNLSE can be solved by the ASSFM, in which we can take into account the variation of fibre parameters with the peak frequency when pulses propagate in the PCF. A general procedure for the ASSFM is presented as follows.

**Step 1** Using PCF parameters $\alpha(\omega_0)$, $\beta_n(\omega_0)$ and $\gamma(\omega_0)$ corresponding to the initial pulse frequency $\omega_0$, we can perform the first-step computation and obtain $A(h,T)$ from $A(0,T)$ by the SSFM.

**Step 2** The pulse spectrum corresponding to $A(h,\ T)$ can be obtained by fast Fourier transform (FFT). Then, the central frequency $\omega_{\mathrm{mid}}(h)$ corresponding to the peak value in the pulse spectrum can be found by a searching algorithm.

**Step 3** Using PCF parameters $\alpha(\omega_{\mathrm{mid}})$, $\beta_n(\omega_{\mathrm{mid}})$ and $\gamma(\omega_{\mathrm{mid}})$ corresponding to $\omega_{\mathrm{mid}}$ obtained in step 2, we can perform computation again and obtain $A(z+h,\ T)$ from $A(z,\ T)$ by the SSFM. In step 2, we can obtain $\omega_{\mathrm{mid}}(z+h)$ corresponding to $A(z+h,\ T)$.

**Step 4** Repeating step 3 we can finally obtain $A(L,\ T)$ and its corresponding frequency spectrum.

Certainly, it is time-consuming to simulate the pulse propagation in PCFs by ASSFM if we change PCF parameters in every step-size $h$. Practically, we need not change the PCF parameters in every step-size but may change PCF parameters in a multi-step manner. In addition, we can utilize the predictor–corrector split-step Fourier method proposed by Liu and Lee[23] to increase the computing speed.

## 3. Numerical results

In our numerical simulation, we consider a PCF, which is made from pure silica with a hexagonal array of air holes running along its length and the central hole missing to form a solid core.[24] The pitch of the fibre is 2.6$\mu$m and the cladding air hole radius is 1.2$\mu$m. In order to describe it conveniently, we call this fibre PCF1. We have simulated the PCF1 parameters by a fast vector method,[20,21] and the results are shown in Fig.1, where the nonlinear coefficient $\gamma$, the effective mode area $S_{\mathrm{eff}}$, and the dispersion coefficients $\beta_1-\beta_6$ as functions of wavelength $\lambda$ are shown. The zero dispersion wavelength $\lambda_{\mathrm{D}}$ of PCF1 is 0.862 $\mu$m. The PCF1 behaviour is in the anomalous dispersion regime when$\lambda>\lambda_{\mathrm{D}}$. From Fig. 1, we can see clearly that the PCF1 parameters change considerably with wavelength variation. Therefore, it is necessary that ASSFM should be used to solve the GNLSE for simulating the pulse propagation and evolution in PCFs.

First, pulse propagation in the PCF1 is simulated by SSFM and ASSFM separately assuming that the sech-pulses with a central wavelength of 1.0$\mu$m, a duration $T_{\mathrm{FWHM}}$ of 100fs, an average power of 46mW, and a repetition rate of 75MHz are transmitted in the PCF1. The corresponding pulses have a peak power of $P_0$=8.814 kW. The temporal and spectral evolutions along the PCF1 are shown in Figs.2 and 3 respectively. It should be noted that the intensity of the spectrum in Fig.3 has been normalized to its peak power and the output is in units of dB.

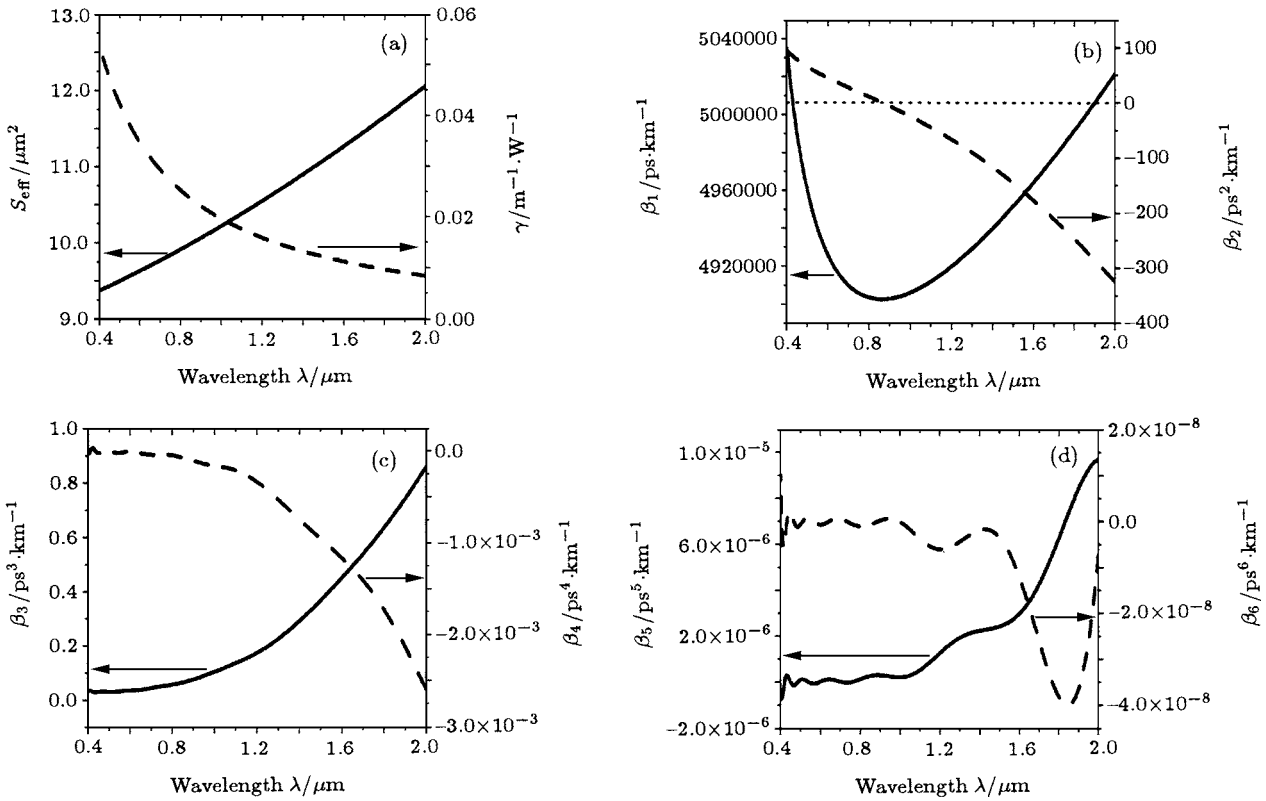



**Fig.1.** Parameters of PCF1 simulated by a fast vector method. (a) Nonlinear coefficient $\gamma$ and effective mode area $S_{\rm eff}$ as functions of wavelength $\lambda$. (b) $\beta_1$ and $\beta_2$ as functions of wavelength $\lambda$. (c) $\beta_3$ and $\beta_4$ as functions of wavelength $\lambda$. (d) $\beta_5$ and $\beta_6$ as functions of wavelength $\lambda$.

By comparison, we can find great differences between the simulated results by the two methods especially for the spectrum in Fig.3. The central wavelength 1.0$\mu$m of the initial pulses lies in the anomalous group velocity dispersion region. The interaction of self-phase modulation (SPM) resulting from the nonlinear refractive index and anomalous group velocity dispersion creates an $N$th-order soliton described by $N^2 = \gamma P_0 T_0^2/|\beta_2|$, where $T_0$ is the input pulse duration. We have computed and obtained the nonlinear length $L_{\rm NL} = 1/(\gamma P_0)$=0.0058m, second-order dispersion length $L_{\rm D} = T_0^2/|\beta_2|$=0.129m, third-order dispersion length $L'_{\rm D} = T_0^3/|\beta_3|$=1.776m, soliton order $N = \sqrt{L_{\rm D}/L_{\rm NL}}$ =4.72, and soliton period $z_0 = \dfrac{\pi}{2}L_{\rm D} = \dfrac{\pi}{2}\dfrac{T_0^2}{|\beta_2|}$= 0.203m by using the PCF1 parameters corresponding to the central wavelength of the initial pulses. Under these conditions, the soliton effect plays an important role in the process of pulse propagation in the PCF. Due to Fourier transform limit, the narrower the pulse duration, the broader the pulse spectrum will be. When pulses propagate in the PCF blue-shifted components in the pulses can act as a pump and can be further shifted into the red spectral region due to Raman self-frequency shift. Furthermore, the contribution from other effects such as the self steepening, Raman effect, third-order or even higher-order dispersion acts as a perturbation and destroys soliton stability and leads to fission of higher-order solitons. Since all solitons and their corresponding non-solitonic radiation (NSR) have different central frequencies, a broadband continuum is generated, which is in agreement with the experimental and theoretical results.[3,4,25–27] In addition, according to the adaptive split-step Fourier theory the PCF parameters $\alpha(\omega)$, $\beta_n(\omega)$ and $\gamma(\omega)$ would change greatly with the frequency of the red-shifted highest peak, which is an instability factor for high-order solitons and results in breaking of high-order solitons with different central frequencies.[28] Once the propagating pulses arrive at a certain distance the superposition of solitons with different central frequencies and the corresponding NSR may form a flattened supercontinuum. From Fig.3(b) a relatively flattened supercontinuum is formed when pulses propagate a distance $z$=6cm and a steady supercontinuum is formed when pulses propagate a distance $z$=8cm in the PCF. The 20 dB spectrum width ranges from $\lambda$ =1.0 to 1.45$\mu$m. From Fig.3(b) we also can see that remarkable blue-shifted radiation appears

in a range from $\lambda$ =0.5 to 0.6$\mu$m, which also confirms the view of higher-order soliton fission to produce red-shifted solitons and blue-shifted NSR.[3,25,26]

From Figs.2(a) and 2(b), one can see that the difference between the results obtained by SSFM and ASSFM increases with increasing distance. The time-delay of the highest peak of simulated temporal evolution by the ASSFM is larger than that by the SSFM and other sub-peaks easily break with increasing distance $z$. From Figs.3 (a) and 3(b), one can see that the difference between the results obtained by the SSFM and ASSFM are more remarkable when the distance increases. Although all the steady supercontinua can be formed by the two methods, wider spectra are obtained by the ASSFM than by the SSFM. For the ASSFM, the frequency corresponding to the pulse peak varies with the transmission distance and as a result the parameters $\beta_n(\omega)$ and $\gamma(\omega)$ also vary with the transmission distance. These variations result in soliton breaking, and make it easier to form a flattened and wider spectrum. Through the above analysis, one can see that the ASSFM must be used in simulating the pulses propagation in the PCF in the case of remarkable soliton self-frequency shift. It is necessary that the ASSFM should be used to solve the GNLSE so that more accurate simulation of pulses propagation and evolution in photonic crystal fibres can be gained.

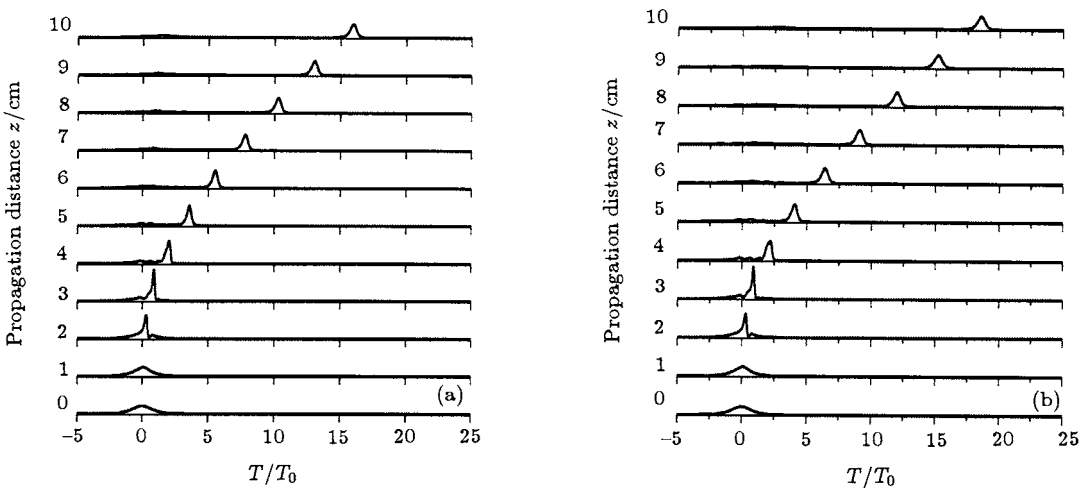



**Fig.2.** The temporal evolution along the PCF1 of the input pulse with central wavelength $\lambda_0$=1.0$\mu$m. (a) The result obtained by SSFM. (b) The result obtained by ASSFM.

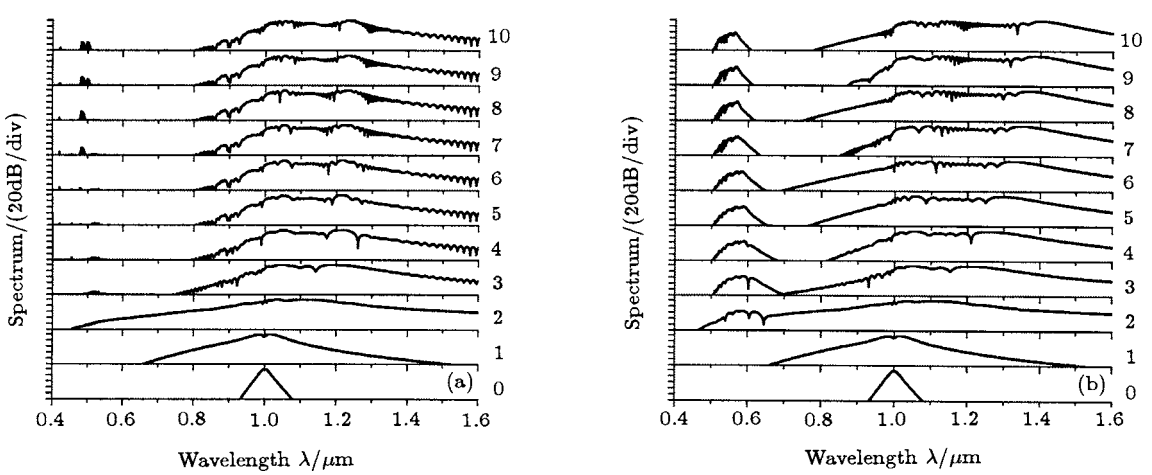



**Fig.3.** The spectral evolution along the PCF1 of the input pulse with central wavelength $\lambda_0$=1.0$\mu$m. (a) The result obtained by SSFM. (b) The result obtained by ASSFM.

Secondly, the pulses, with the same parameters as before but at a central wavelength $\lambda_0$=0.862$\mu$m, propagating in the PCF1 are simulated by the ASSFM in order to examine the influence of dispersion on the pulse propagation. The simulated results are shown in Fig.4. The central wavelength $\lambda_0$=0.862$\mu$m of the initial pulses is the zero dispersion wavelength of the PCF. The PCF1 parameters corresponding to $\lambda_0$=0.862 are used, that is, nonlinear length $L_{\rm NL}$ =0.0049m and the third-order dispersion length $L'_{\rm D}$= 2.75m. SPM and the third-order dispersion play important roles in the initial process of pulse propagation in PCF1. Because the SPM results in spectrum broadening, pulse frequency components extend toward two directions: its red shifted component is situated in the anomalous dispersion region and the blue shifted component is situated in the normal dispersion region. Even if the central wavelength of the initial input pulses is consistent with the zero dispersion wavelength of PCF1, actually the pulse cannot propagate at PCF1's zero dispersion wavelength at all times. Even excitation in the normal dispersion region close to the zero-dispersion wavelength can also create $N$th order solitons in the anomalous dispersion region.[3,25] In practice, $\beta_2$ is determined by the highest peak in the pulse spectrum in the transmission process. The variation of the frequency corresponding to the pulse peak can be taken into account by the ASSFM naturally and accurately, and therefore this method ensures the reliability of the simulated results.

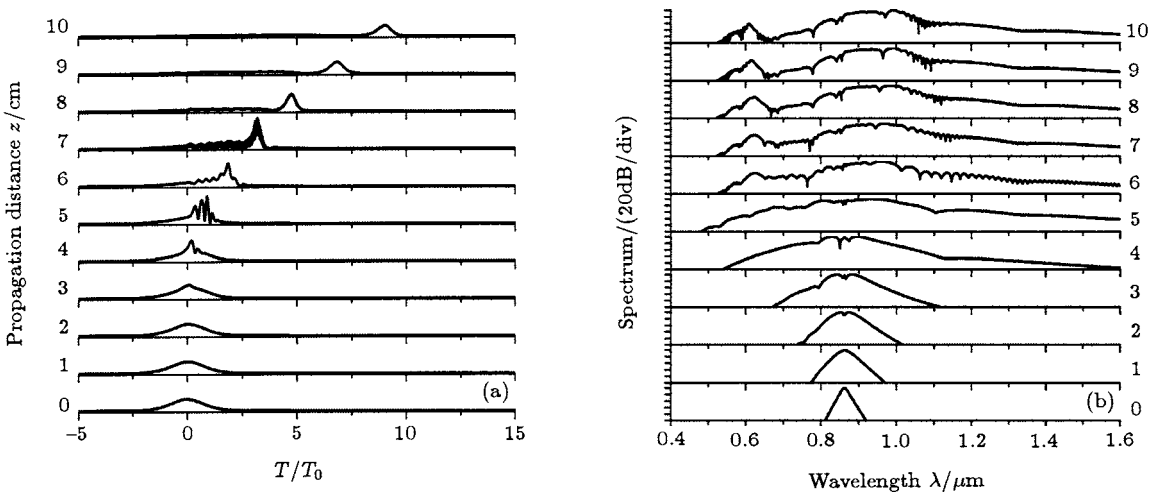



**Fig.4.** Simulated results of pulse propagation in PCF1 at a central wavelength $\lambda_0$=0.862$\mu$m by ASSFM. (a) The temporal evolution along the PCF1. (b) The spectral evolution along the PCF1.

Thirdly, the pulses, with the same parameters as before but at a central wavelength $\lambda_0$=0.8$\mu$m, propagating in the PCF1 are simulated by ASSFM. The longest distance of pulse propagation is $z_{\rm max}$=10cm in the simulation process. The results are shown in Fig.5. The central wavelength $\lambda_0$=0.8$\mu$m of the initial pulses lies in the normal dispersion region of the PCF1. From Fig.1 it can be seen that the nonlinear coefficient $\gamma$ of the PCF1 increases when the wavelength decreases. Under the condition of the same peak power of initial pulses, the SPM plays an important role in the initial process of pulse propagation in the PCF, and the red shifted component moves faster than the blue shifted component in pulses propagating in the normal dispersion region of the PCF. The interaction of the SPM and group velocity dispersion (GVD) leads to spectrum broadening in two directions, namely, creating red and blue shifted components respectively. In addition, the contribution from other effects such as the Raman effect, self steepening and especially third-order dispersion acts as a perturbation and leads to temporal aberrance and frequency chirping. The temporal and spectral results shown in Fig.5 become asymmetric distribution when the propagation distance $z$ increases. The main mechanism of pulse broadening in the PCF's normal dispersion regime is the interaction of the SPM and GVD, and the extent of spectrum broadening is smaller than that in the near-zero dispersion or anomalous dispersion regime.

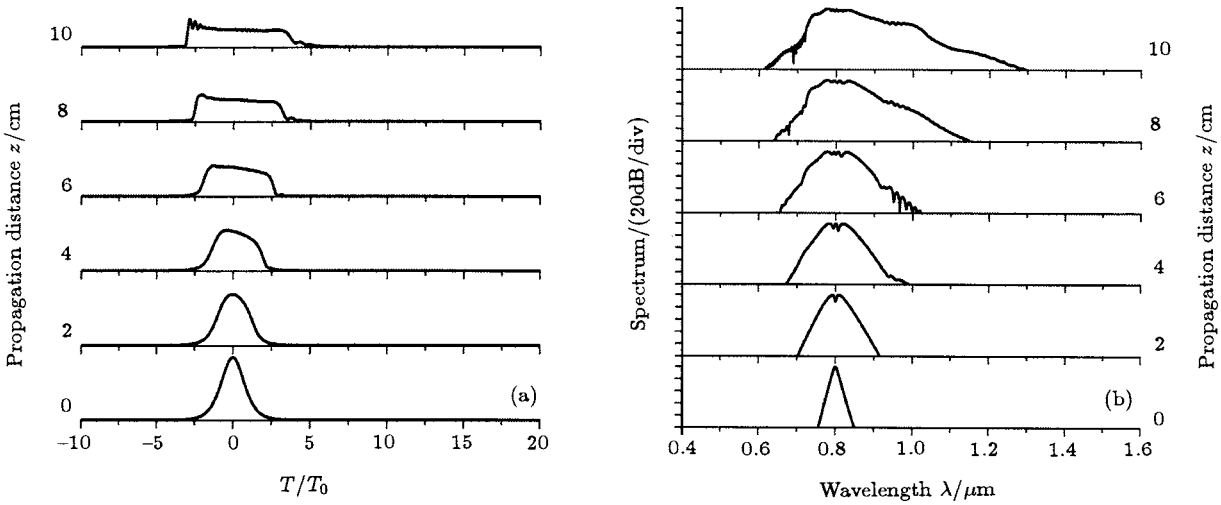



**Fig.5.** Simulated results of pulse propagation in PCF1 at a central wavelength $\lambda_0$=0.8$\mu$m by ASSFM. (a) The temporal evolution along the PCF1. (b) The spectral evolution along the PCF1.

In order to confirm the reliability of the ASSFM, the experimental result reported in Ref.[3] has been simulated by SSFM and ASSFM, and the results are shown in Fig.6 (a). The spectrum of laser pulses is acquired from a microstructured fibre with a length of 15cm, a core diameter of 2.4$\mu$m, an air-filling fraction of 47.3%. Input initial laser pulses with a central wavelength of 800nm, a duration $T_{\mathrm{FWHM}}$ of 100fs, a spectrum width of 12nm and a power of 200 mW are coupled into the fibre in the experiment.[3] Naturally, the same parameters are used in the numerical simulation. Absolute error spectra between the experimental and simulated results are shown in Fig.6(b). From Fig.6(a) we can see that the simulated spectrum by the ASSFM is closer to the experimental result than the spectrum simulated by the SSFM especially in the short wavelength region. From Fig.6(b) we can see that the absolute error from the SSFM is larger than the ASSFM obviously. The microstructure of the fibre used in the experiment[3] is not as regular as the ideal PCF. Therefore the fibre parameters used in the simulation are approximate especially for the high-order dispersion. This is the main reason that explains the difference between simulation and experiment results. From Fig.6 we can see that the ASSFM can be used to solve the GNLSE to improve the simulation precision for pulses propagation in PCFs.

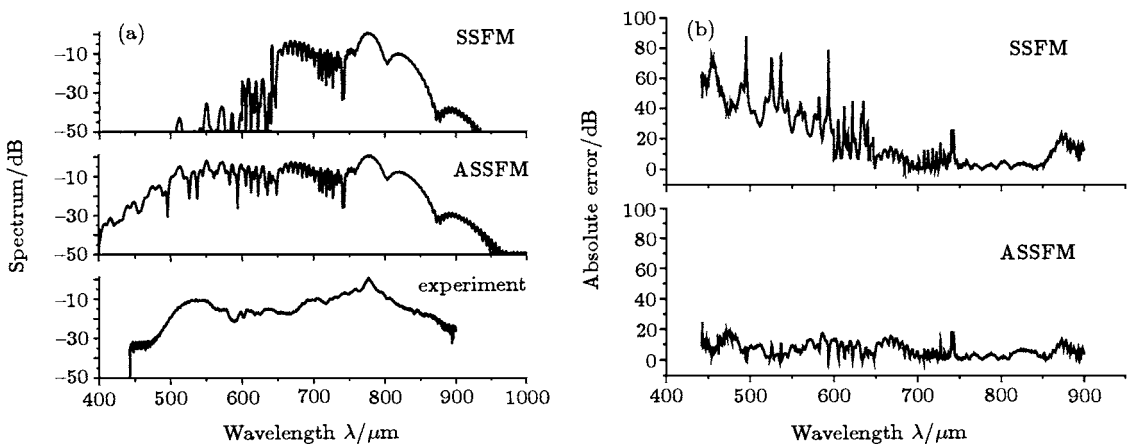



**Fig.6.** (a) Comparison between the experiment spectra reported in Ref. [3] and the simulated spectra by SSFM and ASSFM. (b) Absolute error between experimental spectra and simulated results.

## 4. Conclusion

In summary, based on the traditional SSFM, the ASSFM has been proposed to solve the GNLSE for the first time so far as we know and it can improve simulation precision. The reliability and necessity of the ASSFM have been validated by numerical analysis and comparison with experimental result. It is found that the ASSFM should be used to solve the GNSE to ensure precision when the soliton self-frequency shift is remarkable and the PCF parameters change with the pulse frequency remarkably. The dispersion characteristics of PCFs have strong influence on the spectrum width when the ultrashort pulses propagate and evolve in the PCFs. Even if for the same PCF the mechanism and extent of spectrum broadening have great differences in different dispersion regimes. The precision of numerical simulation by the ASSFM is higher than by the SSFM in the process of laser pulse propagation in PCFs because the variation of fibre parameters with the peak frequency can be taken into account fully.

## References


[1] Coen S, Chau A H L, Leonhardt R, Harvey J D, Knight J C, Wadsworth W J and Russell P St J 2001 *Opt. Lett.* **26** 1356

[2] Zhu Z M, Brown T G 2004 *Opt. Exp.* **12** 791

[3] Li S G , Ji Y L, Zhou G Y and Hou L T 2004 *Acta Phys. Sin.* **53** 478 (in Chinese)

[4] Li S G, Hou L T, Ji Y L and Zhou G Y 2003 *Chin. Phys. Lett.* **20** 1300

[5] Zhu Z M and Brown T G 2004 *Opt. Exp.* **12** 689

[6] Schreiber T, Limpert J and Zellmer H 2003 *Opt. Comm.* **228** 71

[7] Hundertmark H, Kracht D, Wandt D and Fallnich C 2003 *Opt. Exp.* **11** 3196

[8] Nikola I N and Thorkild S 2003 *Opt. Soc. Am.* B **11** 2329

[9] Fang X J, Karasawa N, Morita R, Windeler R S and Yamashita M 2003 *IEEE Photon. Tech. Lett.* **15** 233

[10] Gu X, Kimmel M, Shreenath A P and Trebino R 2003 *Opt. Exp.* **11** 2697

[11] Kumar V V , George A K, Reeves W H, Knight J C and Russell P St J 2002 *Opt. Exp.* **10** 1520

[12] Nicholson J W Yan M F, Wisk P, Fleming J, DiMarcello F, Monberg E and Yablon A 2003 *Opt. Lett.* **28** 643

[13] Hu M L, Wang C Y, Chai L Li Y F, Dukel K V, Khokhlov A V, Shevandin V S, Kondrat Y N and Zheltikov A M 2004 *Laser Phys. Lett.* **1** 299

[14] Hu M L, Wang C Y, Chai L and Zheltikov A M 2004 *Opt. Exp.* **12** 1932

[15] Hu M L, Wang C Y, Li Y F, Wang Z, Ni X C, Chai L, Li S G, Hou L T and Zhou G Y 2004 *Laser Phys.* **14** 776

[16] Qian S X and Wang G M 2001 *Principle and Progress of Nonlinear Optics* (Shanghai, China: Fudan Academic)

[17] Agrawal G P 2001 *Nonlinear Fiber Optics* (London, U.K.: Academic)

[18] Li S G and Yang S D 2002 *Well Logging Tech.* **26** 40 (in Chinese)

[19] Li S G, Liu X D and Hou L T 2003 *Acta Phys. Sin.* **52** 2811 (in Chinese)

[20] Li S G, Liu X D and Hou L T 2004 *Acta Phys. Sin.* **53** 1873 (in Chinese)

[21] Li S G, Liu X D and Hou L T 2004 *Acta Phys. Sin.* **53** 1880 (in Chinese)

[22] Li S G, Liu X D and Hou L T 2004 *Chin. J. Lasers* **31** 713 (in Chinese)

[23] Liu X M and Lee B 2003 *IEEE Photon. Tech. Lett.* **15** 1549

[24] Knight J C, Birks T A , Russell P St J and Atkin D M 1996 *Opt. Lett.* **21** 1547

[25] Husakou A V and Herrmann J 2001 *Phys. Rev. Lett.* **87** 203901

[26] Herrmann J, Griebner U and Zhavoronkov N 2002 *Phys. Rev. Lett.* **88** 173901

[27] Liu X D, Li S G, Guo H L, Zhang D Z, Li Z L and Hou L T 2003 *Chin. Phys.* **12** 1143

[28] Chen X W, Lin X S and Lan S 2005 *Chin. Phys.* **14** 366